Bull. Inst. Chem. Res., Kyoto Univ., Vol. 58, No. 4

Lattice Distortion of Polyethylene at Low Temperatures

Akiyoshi KAWAGUCHI*, Ryoh MATSUI**
and Ken-ichi KATAYAMA*

Received July 5, 1980

The temperature dependence of lattice distortion and crystallite size of polyethylene was discussed from the analysis of the diffraction profile measured over the temperature range from 4.5°K to 300°K. The integral breadth was obtained from the profile using the analytical function composed of the Gaussian and Lorentzian functions. The integral breadth increased with lowering the temperature. This process is reversible. From the fact that the ratio of the integral breadth of 400 reflection to that of 200 one increased at low temperatures, the increase of integral breadth was found to be due mainly to the increase of lattice distortion. The lattice distortion and crystallite size were quantitatively estimated by the method of integral breadth in terms of the micro-strain or paracrystalline disorder. The result showed that the lattice distortion increased with lowering the temperature, while the crystallite size remained almost costant. The shape of line profile transferred from the Gaussian to the Lorentzian with the rise of temperature. This transfer of diffraction profile was interpreted as caused by the change of lattice distortion from the micro-strain of the Gaussian distribution to the paracrystalline disorder.

KEY WORDS: Line profile/ Integral breadth/ Micro-strain/ Paracrystalline disorder/ Crystallite size/ Low temperature/

INTRODUCTION

The study on polymer solid at low temperatures is motivated not only by the intellectual curiosity towards the structure and property of polymers in the cryogenic state but also by its applicability as material to cryogenic systems, especially in relation with space research.[1] Though quantitative as well as qualitative investigations have been made on various polymers, better understanding of polymer solid requires the knowledge on its structure in atomic or molecular level at low temperatures through methods as X-ray, electron and neutron diffractions. Katayama has pioneered the low-temperature investigation on the structure of polyethylene by X-ray diffraction.[2] Then followed the work on thermal motion and lattice imperfection by Kilian.[3] In these works, however, the temperature range is limited to 77°K at lowest where some modes of molecular motions remain active as expected from the δ relaxation process below 77°K.[4] The standard of the structure and property of polymer solid is to be given from its study in the state where all the molecular motions are frozen. Liquid helium is an available cooling medium for this purpose. Most of works with liquid helium reported so far are concerned with molec-

* 河口昭義, 片山健一: The Institute for Chemical Research, Kyoto University, Uji, Kyoto-Fu 611, Japan
** 松居りよう: Technical Research Laboratory, Asahi Chemical Industry Co. Ltd., Fuji, Shizuoka-ken 416, Japan

ular motions, *i.e.* the mechanical, dielectric or magnetic relaxation and the measurement of specific heat. The first X-ray diffraction experiment with liquid helium (10°K) is on the cell dimension of polyethylene crystal by Shen *et al.*[5] The lattice distortion of polyethylene crystal has been measured at 15°K by Höhne and Wilke.[6] The precise structure analysis of polyethylene at liquid helium temperature was carried out by Abitabile *et al.* with neutron diffraction[7] and Kawaguchi *et al.* with X-ray diffraction.[8] Succeeding to our last work, we will here discuss the structure of crystalline polyethylene at low temperatures in terms of lattice distortion or imperfection.

EXPERIMENTAL

An unfractionated linear polyethylene Sholex 6050 (produced by Showa Denko K.K.) was used as a starting material. Single crystals were isothermally grown from its 0.05 wt% solution in *p*-xylene at 80°C. The sedimented mats of single crystals were prepared by the filtration of crystals suspending in solvents. The polyethylene was also crystallized from the melt at 129°C and its oriented specimen was prepared by drawing a strip of bulk sample to several times its original length at 90°C and by annealing at 120°C.

Since single crystals were slightly oriented in the sedimented mat, crystalline powder was prepared by crushing and grinding the brittle mat at liquid nitrogen temperature. The X-ray diffraction pattern of the powder thus prepared was measured at low temperatures and used for the analysis of the crystal structure and lattice distortion. The structure was analysed by means of the least squares method.[8-10]

The X-ray diffraction apparatus suitable for the diffractometrical measurement at low temperatures was manufactured by Rigaku-Denki Co. Ltd.

FUNDAMENTALS OF DATA ANALYSIS

Broadening of the X-ray diffraction profile arises from the fact that a diffraction specimen is composed of small crystallites and/or that the crystal lattice is strained or distorted. In the diffraction theory, the former is expressed in terms of the shape factor $|S(\mathbf{s})|^2$ which is the square of the Fourier transform of a function expressing a crystalline domain and the latter in terms of the lattice factor $Z(\mathbf{s})$ which is the Fourier transform of the coordination statistics of lattice points in a crystal. Here, $\mathbf{s}$ is the reciprocal vector. The line profile is given by the convolution of the two factors;

$$Z(\mathbf{s}) * |S(\mathbf{s})|^2 \tag{1}$$

where the symbol $*$ denotes the operation of convolution. The determination of crystallite size and lattice distortion or strain requires the separation of the contribution of these two factors to line profiles. Several methods have been proposed for this purpose: (1) the Fourier method of Warren and Averbach is most excellent as an analytical method,[11] (2) the use of variance was developed for the profile analysis by Wilson[12] and (3) the use of the integral breadth was found to be useful empirically[13] and its theoretical development was done by Wilson[14] and by Wilson and Stokes.[15] Following these works, many researchers have carried out the profile analysis of diffraction pattern.[16] Originally, these methods have been developed and advanced to investigate the crystalline nature of

cold-worked metals. Another treatment based on the 'paracrystal concept' has been put forward by Hosemann.[17] The paracrystalline theory is of practical use for the determination of the crystallite size and distortion of crystalline polymer solid in which the disorder of long range (or the disorder of the second kind) is significant. Buchnan and Miller applied these methods to the determination of the crystallite size and distortion of isotactic polystyrene and discussed the difference in results obtained by respective methods.[18] The detailed comparison of these methods should be referred to the textbook by Klug and Alexander.[19]

The observed diffraction profile is broadened by instrumental factors and affected by various kinds of random noises. Thus the data analysis of this broadened profile includes two procedures; (1) the extraction of the pure diffraction profile of the specimen from an as-measured diffraction pattern and (2) the determination of the crystallite size and lattice distortion from the pure diffraction profile.

1. A choice of method for the determination of crystallite size and lattice distortion.

The Fourier and variance methos are preferred to the method of integral breadth, since they can be applied without assuming any specific model on the distribution of crystallite size and the nature of lattice distortion. In these methods, the accuracy depends on the reliability of the extracted pure diffraction profile. Especially its tail is of primary importance, because in the Fourier method the coefficients of the harmonics of low order of the profile are very sensitive to the tail and in the variance method the tail deterimines the limit of integration on which the variance of line profile largely depends. Therefore, in the actual procedure of line profile analysis, the back ground level of as-measured pattern should be estimated with upmost care. The back ground level could be well defined in such a sharp diffraction pattern as that of metal or inorganic material. However, the diffraction profile of crystalline polymer solid is inherently broad and tails over a wide range. Since the tail of such an irregular pattern smears gradually into the back ground, its tracing is difficult and its trace end cannot be estimated correctly. Thus the separation of diffraction profile from the back ground inevitably involves some ambiguity. Integral breadths are not so sensitive to the choice of back ground level. From the experimental point of view, the method of integral breadth is superior to the Fourier or variance method, though a model of lattice distortion should be assumed in advance and the result is somewhat influenced by its choice in the method of integral breadth.

Methods of analysis by integral breadth

The method of integral breadth is adopted here for the profile analysis. Since only two reflections—200 reflection and its higher order reflection (400)—are practically available, the information obtained by this method is restricted in quantity and in quality. Accordingly, a complicated assumption in analysis may be of little value. Let us proceed with the analysis of line profile on the assumption *that the shape and lattice factors are approximated by an analytical function—the Gaussian or Lorentzian function.* Then, the convolution of (1) is reduced to a simple expression and the following relations as to the integral breadth are derived.

$$\beta^2=(\lambda/\bar{D}\cos\theta)^2+(2\eta(h,o)\tan\theta)^2 \qquad (2)$$

(Gaussian—Gaussian)

$$\beta=\lambda/\bar{D}\cos\theta+2\eta(h,o)\tan\theta \tag{3}$$
(Lorentzian—Lorentzian)

in the case of the micro-strain-type of distortion,[15] and

$$\beta'^2=1/\bar{D}^2+(\pi gm)^4/\bar{d}^2 \tag{4}$$
(Gaussian—Gaussian)

$$\beta'=1/\bar{D}+(\pi gm)^2/\bar{d} \tag{5}$$
(Lorentzian—Lorentzian)

in the case of paracrystalline disorder.[17] The first and the second terms in the right side of these equations show the contribution of the shape and lattice factor, respectively. β and β' denote the integral breadths in radians and in Å^{-1} respectively, λ the wavelength of X-ray, $\bar{D}$ the average crystallite size, $\eta(h,o)$ the 'apparent strain' equal to $2.5\langle\varepsilon^2\rangle^{1/2}$ ($\langle\varepsilon^2\rangle^{1/2}$ is the root-mean-square strain) in the direction h, θ the Bragg angle of the plane, g the paracrystalline disorder $\Delta d/\bar{d}$, $\bar{d}$ the lattice spacing and m the order of reflection.

2. The curve resolution

An as-measured diffraction pattern is the convolution of the pure diffraction pattern of sample with the instrumental broadening. When the instrumental broadening is known, the pure diffraction pattern can be deconvoluted from a measured diffraction pattern by the Fourier transform[20] or by the iterative convolution.[21] Though an extensive computation will be involved, these deconvolution procedures can be handled with a computer if a smoothed diffraction profile with high S/N is obtainable. Since such a smooth diffraction pattern can be hardly obtained, the method of integral breadth in which the pure diffraction profile is not needed is adopted here for the determination of crystallite size and lattice distortion.

Determination of the integral breadth

The diffraction profile is usually approximated by the analytical expression consisting of the Gaussian and Lorentzian function so that its integral breadth is given in terms of the breadth of the composed function.[22] The Gaussian function is expressed by

$$g(x,A,W,P)=A\cdot\exp\left(-ln\left(2(x-P)/W\right)^2\right) \tag{6}$$

and the Lorentzian function by

$$h(x,A,W,P)=A/\left(1+(2(x-P)/W)^2\right) \tag{7}$$

where x corresponds to a diffraction angle 2θ and the parameters A, W and P denote the peak height, half-value width and peak position of a diffraction peak, respectively. The pure diffraction profile can be well approximated by the weighted sum of the two component functions as follows;

$$f(x,A,W,P)=(1-C)g(x,A,W,P)+C\cdot h(x,A,W,P) \tag{8}$$

where C is the fraction of Lorentzian component. The real X-ray is composed of the doublet of $K\alpha_1$ and $K\alpha_2$ even after the filtration of K_β or the monochromatization, and eq. (8) is thus modified into eq. (9) assuming that the ratio of intensities of $K\alpha_1$ and $K\alpha_2$ is 2:1.

$$f_d(x, A, W, P)=\frac{2}{3}f(x, A, W, P)+\frac{1}{3}f(x+\Delta x, A, W, P) \tag{9}$$

where Δx is the increment of diffraction angle for $K\alpha_2$ from that for $K\alpha_1$. Instrumental broadening itself can also be estimated from eq. (9). A well-annealed silver powder was used as a standard material for the correction of the instrumental broadening. After a diffraction profile of silver powder, *e.g.* the 220 reflection profile, was normalised in such a way that its integral intensity was unity, the parameters A, W and P in eq. (9) fitting to the profile were estimated by the least squares method in order to obtain the function for the instrumental broadening, f_i. The back ground intensity is expressed by

$$f_b(x)=ax^3+bx^2+cx+d \tag{10}$$

where a, b, c and d are constants. The diffraction profile where j peaks overlap can be expressed by the following equation.

$$F_c(x)=\sum_j f_{d,j}*f_i+f_b \tag{11}$$

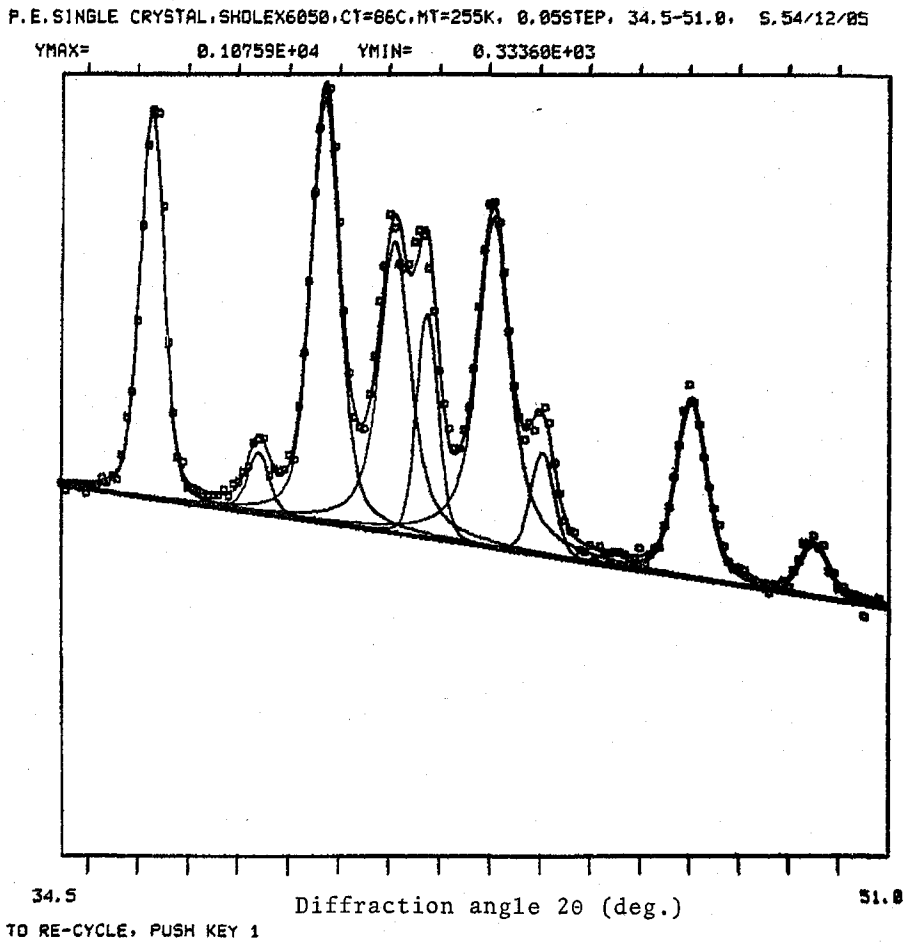

Fig. 1. The peak separation of the diffraction profile. The result is after three iterations of least squares procedure. Symbol □ shows the observed data.

Then, the integral breadth of jth peak is expressed by

$$\beta_j=\frac{1}{2}(C_j\sqrt{\pi/\ln 2}+(1-C)\pi)W_j \tag{12}$$

The fitting of eq. (11) to the observed pattern was carried out with a computer by means of the least squares method to minimize the following R value;

$$R=\sum_i w_i(F_c(x_i)-F_0(x_i))^2 \tag{13}$$

where $F_c(x_i)$ and $F_0(x_i)$ are the diffraction intensities calculated by eq. (11) and observed at x_i, respectively, and w_i the weight for the intensity. Figure 1 shows an example of this analysis.

RESULTS AND DISCUSSION

Disorder of the first kind at low temperatures

The crystal structure of polyethylene single crystal at 4.5°K was analysed by the least squares method on the basis of the intensity data of the powder diffraction. The cell dimensions and lattice parameters are shown in Table I and compared with those of melt grown crystal reported previously[8]. The unit cell of single crystal expands in the direction

Table I. The observed lattice parameters of single and melt-grown polyethylene crystals.

Unit cell dimensions (Å)			
a	b		c
7.16_8	4.88_0		2.55_2
(7.12_8)	(4.85_2)		(2.55_3)
Co-ordinates of carbon atom			
x/a	y/b		z/c
0.04_4	0.06_1		0.25
(0.04_6)	(0.06_5)		0.25
Temperature factors (Å^2)			
B_{11}	B_{22}	B_{33}	B_{12}
0.02_7	0.03_3	0.04_6	-0.01_1
(0.01_2)	(0.02_5)	(0.07_6)	(-0.001)
Setting angle (deg.)			
47°			
(45.5 ± 3)			
Mean squared displacement (Å^2)			
$<\Delta a^2>$	$<\Delta b^2>$		$<\Delta c^2>$
0.07_1	0.04_0		0.01_5
(0.03_2)	(0.03_0)		(0.02_5)

Values in parentheses denote those of melt-grown crystal.

of both a and b axes and the atomic position of carbon is more tilted toward the a axis, *i.e.* the setting angle which the plane containing the molecular planar zigzag makes with the b axis becomes large. Lamellar crystals have a larger setting angle, when their crystallite size is smaller and when they are thinner and more distorted.[23] The single crystal is thinner and smaller in crystallite size than the melt-grown crystal and its crystal lattice is more distorted. This reflects in the large setting angle of single crystal. Although single and melt-grown crystals are composed of folded chains, the direction of chain folding differs between the two crystals, that is, [110] for the single crystal and [010] for the melt-grown crystal. This difference must be taken into account in comparing the structure and physical state of respective crystals.[24]

Although 4.5°K is not low in the field of low temperature physics, this temperature may well be approximated to the absolute zero point from the viewpoint of thermal motions. Most of molecular motions other than the zero point vibration may be frozen at this temperature. Thus the disorder of the first kind which is obtained from the so-called temperature factors is considered to be due almost to the lattice imperfections rising from the statistical displacement of molecules from the lattice point except the zero point vibration. Therefore, the temperature factors at that cryogenic temperature must be defined as the 'disorder factors'. The disorder factor B_{11} and B_{22} of single crystals are larger than those of melt-grown crystals. This shows that molecular chains displace with larger fluctuation in the a and b directions within single crystals than in melt-grown crystals.

Figure 2 shows the temperature dependence of the relative integral intensity of 020 reflection. The intensity increases with lowering the temperature and decreases in the heating process. This change in intensity with temperature is reversible. Since the 020 reflection stands alone from other reflections and is rather intense, the intensity was measured with high accuracy. Thus the typical data is shown in Fig. 2. Other reflections have the similar behavior of change in intensity with temperature. Crystalline polymer solid is composed of small crystallites interlinked with amorphous chains, so that the

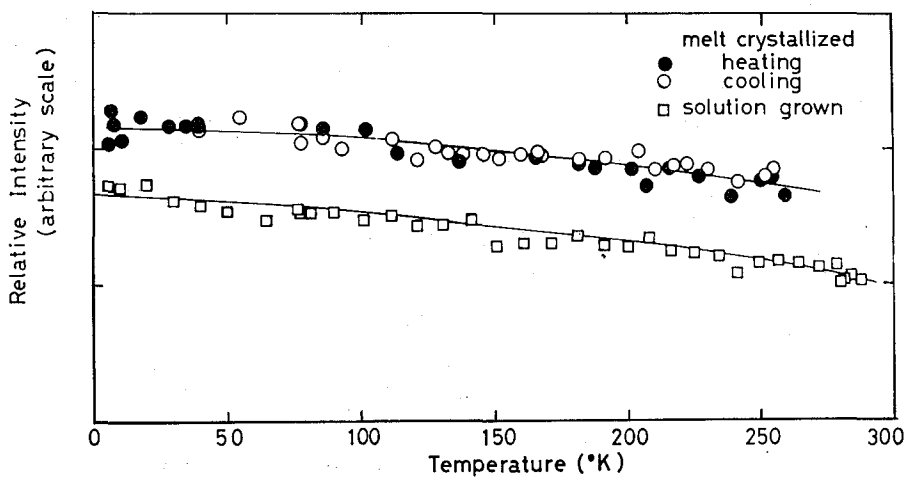

Fig. 2. The relative intensity of 020 reflection as a function of temperature. Symbols ● and ○ show the intensity of melt-grown crystal in heating and cooling processes, respectively. Symbol □ shows the intensity change of single crystal and is shifted downward to such an extent that it is discernible from above ones. The scale of intensity is arbitrary.

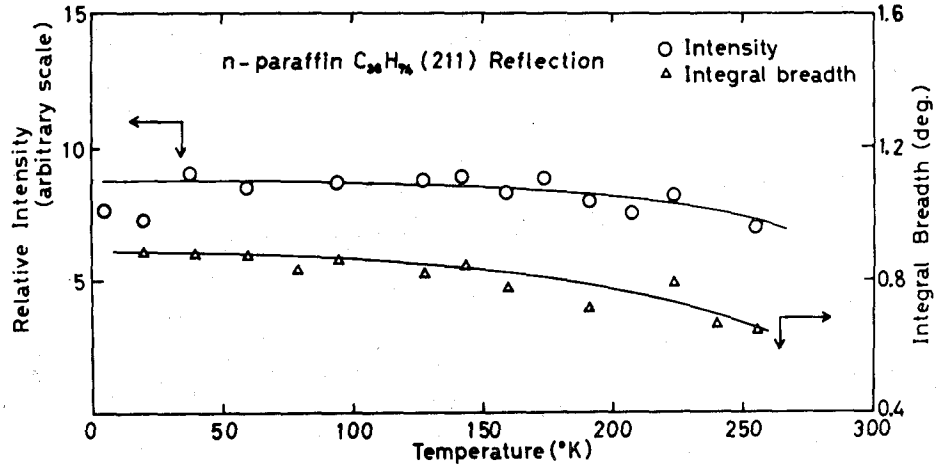

Fig. 3. The relative intensity and integral breadth of 211_s reflection (s denotes the subcell) of n-$C_{36}H_{74}$ crystal with the orthorhombic form. The scale of intensity is arbitrary.

change of reflection intensity with temperature is assumed to be due to the change of the degree of crystallinity, *i.e.* the increase in intensity with the crystallization of amorphous chains or the decrease with melting. According to Kilian's measurements below room temperature, the change of the degree of crystallinity with temperature is very small and thus the crystallization or melting is not expected to cause such a large intensity change as shown in Fig. 2. Figure 3 shows the temperature dependence of the reflection intensity and the integral breadth of $C_{36}H_{74}$ paraffin crystal. Though not to large an extent as in the case of polyethylene, the temperature dependence of the intensity shows the same tendency. Since paraffin has no amorphous chains to crystallize further as polyethylene, this intensity change must be caused by the change in thermal motion of paraffin chains within a crystal. The intensity change with temperature is thus concluded to be due to the thermal motions of molecular chains in the case of polyethylene. The displacement of molecular chains from the lattice point resulting from the thermal agitation is estimated from this intensity change. When the diffraction intensity of the crystal in the state of the 'frozen molecular motion' is known, the fluctuation of atomic position by thermal motion is readily seen from the ratio of the intensity at any temperature to the low temperature intensity.[25,26] This subject will be discussed elsewhere.

Temperature dependence of the integral breadth

The temperature dependence of the integral breadth of 020 reflection for the single and melt-grown crystals is shown in Fig. 4. The integral breadth of both crystals increases with lowering the temperature. This process is reversible. Other reflections also behave in the similar way. As seen in Fig. 3, the identical temperature dependence is observed on the integral breadth of paraffin crystals, although the change is not so large as in the case of polyethylene. Figure 5 shows the reflection intensity and integral breadth of 220 reflection of well-annealed silver powder as a function of temperature. The reflection intensity behaves in the same way with respect to temperature as in polyethylene and paraffin. As predicted from the diffraction theory, the change in thermal motions of atoms in crystals is reflected in the change in intensity. The integral breadth for silver powder is

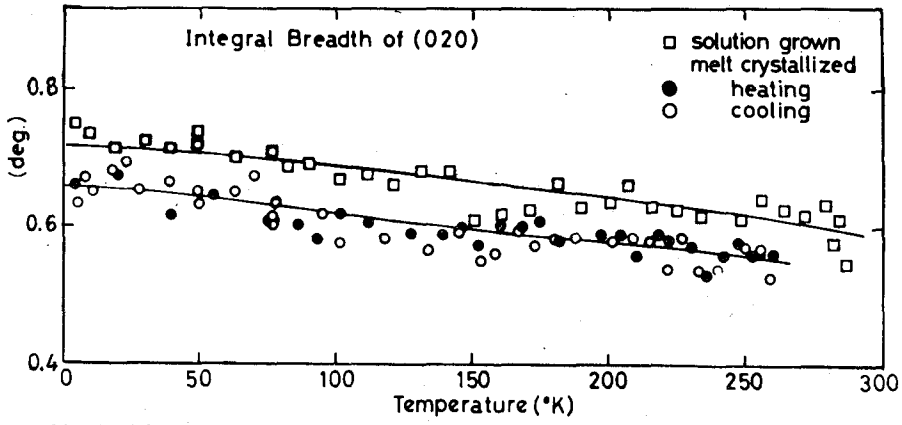

Fig. 4. The temperature dependence of the integral breadth of 020 reflection obtained from Fig. 2. Symbols ● and ○ show the changes of integral breadth of melt-grown crystal in heating and cooling processes, respectively. Symbol □ shows the change of single crystal.

independent of temperature unlike that of paraffin and polyethylene. This may suggest that the increase of integral breadth at low temperatures is characteristic of crystals consisting of long chain molecules such as paraffin and polyethylene. This characteristic was first observed on crystalline polyethylene by Katayama and was called 'the elastic strain' because of the reversibility with temperature.[2)]

Broadening of the diffraction profile is caused by the smallness of crystallite in size and/or the disorder of the second kind—paracrystalline disorder and micro-strain of lattice—and it is independent of the disorder of the first kind. Accordingly, the increase of the integral breadth at low temperatures is caused by the decrease of crystallite size by

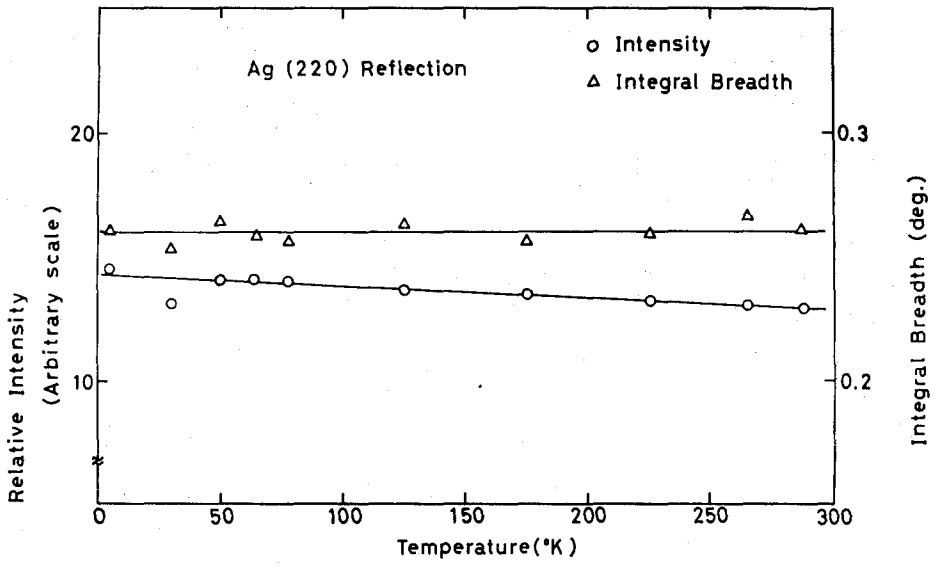

Fig. 5. The temperature dependence of the relative intensity and integral breadth of 220 reflection of well-annealed silver powder. Symbol ○ shows the relative intensity and the scale is arbitrary. Symbol △ shows the change of integral breadth with temperature.

subdivision and/or the increase of the disorder of the second kind. When a crystal lattice is regular, the integral breadth is defined in terms of the Scherrer relation (which corresponds to the first term of the right side of eqs. (2) and (3))

$$\beta=\lambda/\bar{D}\cos\theta \tag{14}$$

When the crystallite size is very large, the effect of micro-strain on the diffraction profile is expressed by the following equation where the integral breadth is given by the second term of the right side of eqs. (2) and (3).

$$\beta=2\eta\tan\theta \tag{15}$$

Thus the broadening of line profile can be attributed to either cause according to the dependence of integral breadth on the order of reflection. Figure 6 shows the ratio of the observed integral breadth of 400 reflection to that of the lower order reflection (200), *i.e.* β_{400}/β_{200}. When only the crystallite is not distorted with temperature, that ratio is equal to the ratio of $\cos\theta_{200}/\cos\theta_{400}$ acoording to eq. (14). The lower dotted line corresponds to the ratio of $\cos\theta$. By contrast, when the crystallite size is very large, the ratio of these two integral breadths whose change is caused by the lattice strain equals that of $\tan\theta_{400}/\tan\theta_{200}$ according to eq. (15). The upper line represents the ratio of $\tan\theta$. Since the observed integral breadth includes the contributions of both crystallite size and lattice distortion, each effect on it can not be separated only by taking account of the ratio of $\tan\theta$ or $\cos\theta$. However, it is possible to distinguish which effect is eminent by ascertaining whether the ratio of the observed integral breadths of the reflections of two different orders changes as that of $\tan\theta$ or $\cos\theta$. Here, the ratio β_{400}/β_{200} becomes closer to the ratio of $\tan\theta$ at lower temperature. This trend suggests that broadening of diffraction profile at low temperatures arises from the increase of lattice distortion or strain rather than from the

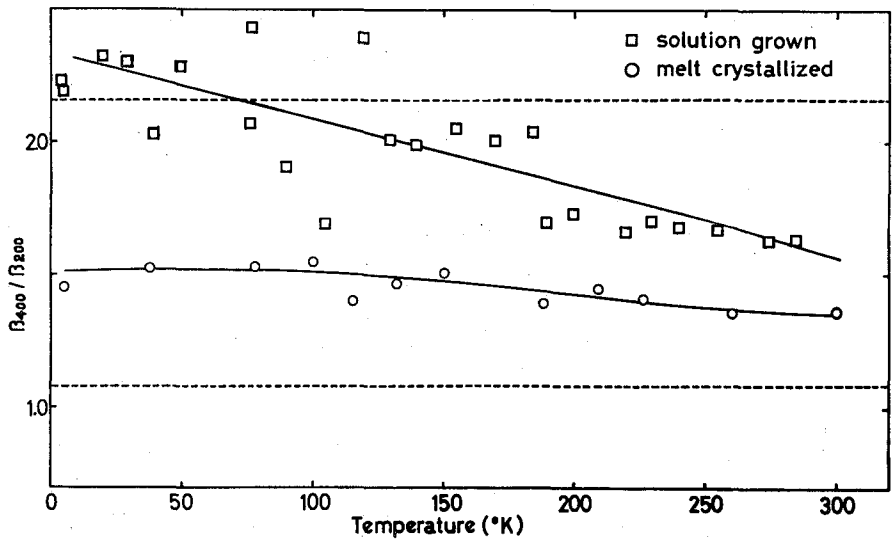

Fig. 6. The ratio of the observed integral breadth of 400 reflection to that of 200 one as a function of temperature. The upper dotted line shows the ratio $\tan\theta_{400}/\tan\theta_{200}$ and the lower line the ratio of $\cos\theta_{200}/\cos\theta_{400}$. Symbols □ and ○ show the results of single and melt-grown crystals, respectively.

decrease of crystallite size.

By analysing the integral breadth of $hk0$ reflections, the above discussion is limited to the disorder of crystal lattice or the crystallite size in the direction normal to the molecular axis. Let us turn our attention to the disorder in the direction parallel to the molecular axis. The analysis of the line profile of 002 reflection is suitable for this purpose. The temperature dependence of 002 reflection of drawn polyethylene was studied here. Since the diffraction profile of single and melt-grown crystals was the Debye-Sherrer pattern, the 002 reflection overlapped other reflections, so that the 002 peak could not be separated accurately from them. Figure 7 shows the integral intensity and integral breadth of that reflection as a function of temperature. As shown above, the intensity decreases with the rise of temperature. From this decrease, it is understood that the thermal displacement of molecular chains or chain segments in the direction parallel to their axis is active at high temperatures. On the other hand, the integral breadth remains constant over the temperature range of observation. This shows that the crystallite size in the direction of molecular axis does not change with temperature and that the disorder of the second kind (perhaps the molecular chains have this disorder in their direction) does not increase with temperature. Since chains are tightly linked by covalent bonds, the long range order of the atomic arrangement in the molecular direction cannot be destroyed by thermal agitation in the crystalline state where fully extended chains are closely packed.

Lattice distortion and crystallite size

From the preceding consideration in terms of lattice strain, it is found that broadening of diffraction profile at low temperatures is due mainly to the increase of lattice distortion. The quantitative analysis of crystallite size and lattice distortion is necessary for further discussion. Equations for this purpose are given in eqs. (2)–(5). These are to be used properly according to the nature of distortion and its distribution. When at least three orders of reflection are available, the most suitable equation is selected out of them and besides the nature of lattice distortion can be defined. Since only two orders of reflection were available in the present work, the best equation could not be determined and therefore

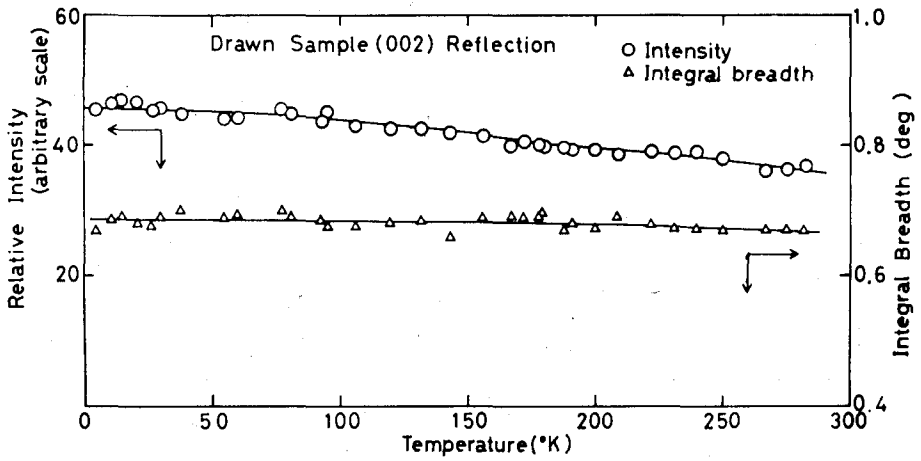

Fig. 7. The temperature dependence of the integral breadth and relative intensity of 002 reflection of drawn polyethylene. Symbols △ and ○ show the integral breadth and relative intensity, respectively.

all the equations were adopted to proceed with the quantitative analysis of crystallite size and lattice distortion. Figure 8 shows the results thus obtained for single crystals. The size of crystallite remains almost constant over the observed range of temperature. On the other hand, g value of paracrystalline disorder and η value of micro-strain increase at low temperatures. The changes of these values for melt-grown crystals are small. Kilian first reported that g value was larger at liquid nitrogen temperature than at room temperature. Höhne and Wilke obtained the same result from the measurement at 15°K. Since the thermal motion of molecular chain is restricted at low temperatures, the crystal is expected to be more perfect. As shown in the present analysis, however, the crystal becomes more distorted with lowering the temperature. This is in conflict with the observation by Schmidt and Vogel that the lattice distortion of polyethylene does not always decrease with the increase of temperature above room temperature.[27]

The line profile is expressed by the convolution of the shape and lattice factors and depends largely on the shape of broadening due to each factor. It is shown that the change of line profile with temperature is caused mainly by the change of the lattice factor, because the lattice distortion varies largely with temperature. The shape of line broardening due to the lattice factor depends on the nature of lattice distortion, *i.e.* the type of distortion and its distribution within a crystal. The relation between the shape of line profile and the nature of lattice distortion is roughly classified in Table II. When the change in the shape of line profile with temperature is known, the change of the nature of lattice distortion is deduced, though roughly, on the basis of Table II. When the diffraction profile is approximated by eq. (8), the fraction of Lorentzian component C serves as an indicator of the shape of profile. Figure 9 shows the change of C for 020 reflection with temperature. The value of C decreases and the profile becomes closer to the Gaussian at low temperatures. This change is interpreted in terms of (1) the change of strain distribution in the case of microstrain and (2) the change of the type of disorder as follows.

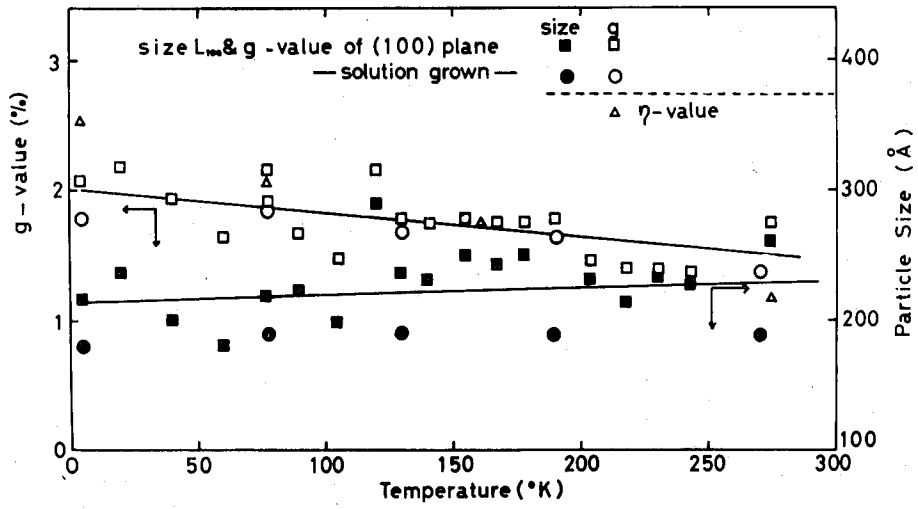

Fig. 8. The temperature dependence of the lattice distortion and crystallite size of single crystal. Symbols ● and ○ show the crystallite size and lattice distortion (g value) obtained by eq. (4), respectively. ■ and □ show the crystallite size and g value obtained by eq. (5). η shows the value obtained by eq. (3).

Table II. Relation between the strain distribution and the shape of line profile.

type of disorder	distribution	line profile
micro-strain	Lorentzian	Lorentzian
	Gaussian	Gaussin
paracrystal	Lorentzian	quasi-Lorentzian
	Gaussian	

(1) In the case of micro-strain, the strain distribution corresponds directly to the shape of line profile as seen in Table II, *i.e.* when the strain distribution is Gaussian, the line profile is also Gaussin and when Lorentzian, it is Lorentzian. This relation shows that the strain distribution in a crystal is represented as Gaussian at low temperatures and as Lorentzian at high temperatures.

(2) When the disorder is paracrystalline, the diffraction profile is quasi-Lorentzian independently of the type of the distribution of disorder. Thus the transfer of the diffraction profile from the Gaussian to the Lorentzian with the increase of temperature is due to the change of the micro-strain of the Gaussian distribution to the paracrystalline disorder.

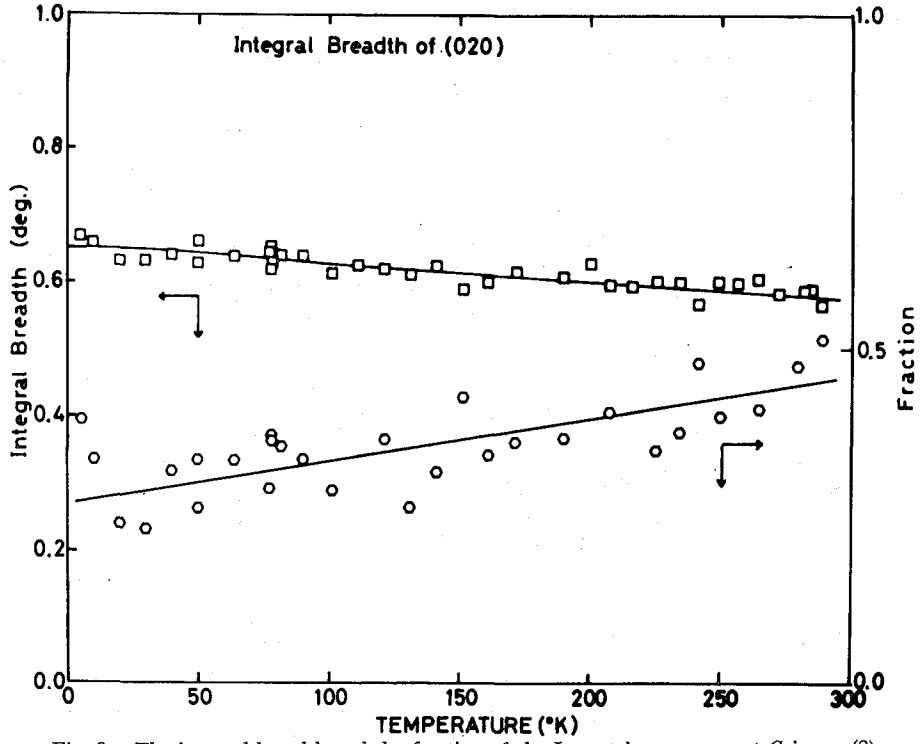

Fig. 9. The integral breadth and the fraction of the Lorentzian component C in eq. (8) of single crystal as a function of temperature. Symbols □ and ○ denote the integral breadth and the fraction of Lorentzian component.

From this simplified consideration, it is sure that the lattice distortion at low temperatures is of micro-strain nature, because the paracrystalline disorder never gives the Gaussian line profile. The paracrystalline disorder differs from the micro-strain in the long range order. The long range order is lost in paracrystals, while it is still retained in elastically strained crystals owing to the internal stress imposed with cooling. Thus, the reversibility of distortion in the course of temperature change is explained by the imposition or removal of elastic strain. By assuming the superposition of micro-strain and paracrystalline disorder, the paracrystalline disorder will be concealed under the dominant micro-strain at low temperatures. When the micro-strain decreases with the relaxation of strain at high temperatures, the paracrystalline nature comes out. This accounts for the decrease of lattice distortion at high temperatures. The present consideration is speculative and it is necessary for the detailed discussion that the profile analysis is carried out by the Fourier or variance method on the basis of accurate data.

REFERENCES

(1) For example, see "Polymers in Space Research", edited by C. L. Segel, M. Shen, and F. N. Kelley, Marcel Dekker, *Inc.*, New York, 1970.
(2) K. Katayama, *J. Phys. Soc. Japan*, **16**, 462 (1961).
(3) H. G. Kilian, *Kolloid-Z.u.Z. Polymere*, **185**, 13 (1962).
(4) Y. S. Papir and E. Baer, *J. Appl. Phys.*, **42**, 4667 (1971).
(5) M. Shen, W. N. Hansen, and P. C. Romo, *J. Chem. Phys.*, **51**, 425 (1969).
(6) G. Höhne and W. Wilke, *Kolloid-Z.u.Z. Polymere*, **241**, 994 (1970).
(7) G. Avitabile, R. Napolitano, B. Pirozzi, K. D. Rouse, M. W. Thomas, and B. T. Willis, *J. Polymer Sci. Polymer Letter*, **13**, 351 (1975).
(8) A. Kawaguchi, R. Matsui, and K. Kobayashi, *Bull. Inst. Chem. Res., Kyoto Univ.*, **55**, 217 (1977).
(9) K. Iohara, K. Imada, and M. Takayanagi, *Polymer J.*, **3**, 357 (1972).
(10) S. Kavesh and J. M. Schults, *J. Polymer Sci., A-2*, **8**, 243 (1972).
(11) B. E. Warren and B. L. Averbach, *J. Appl. Phys.*, **21**, 595 (1950).
(12) A. J. C. Wilson, *Proc. Roy. Soc.* (*London*), **80**, 286 (1962).
(13) W. H. Hall, *Proc. Roy. Soc.* (*London*), ***A*62**, 741 (1949).
(14) A. J. C. Wilson, "X-ray Optics", Mathuen, London, 1949.
(15) A. R. Stokes and A. J. C. Wilson, *Proc. Roy. Soc.* (*London*), **56**, 174 (1944).
(16) F.R.L. Schoening, *Acta Cryst.*, **18**, 975 (1965); W. Ruland. *Acta Cryst.*, **18**, 581 (1965); D. R. Buchnan, R. L. McCullough, and R. L. Miller, *Acta Cryst.*, **20**, 922 (1966).
(17) R. Hosemann and S. N. Bagchi, "Direct Analysis of Diffraction by Matter", North Holland, Amsterdam, 1962.
(18) D. R. Buchnan and R. L. Miller, *J. Appl. Phys.*, **37**, 4003 (1966).
(19) H. P. Klug and L. E. Alexander, "X-ray Diffraction Procedure", 2nd ed., John Wiley and Sons, New York, 1974.
(20) A. R. Stokes, *Proc. Roy. Soc.* (London). ***A*61**, 382 (1948).
(21) S. Ergan, *J. Appl. Crystallogr.*, **1**, 19 (1968).
(22) A. M. Hindeleh and D. J. Johnson, *Polymer*, **13**, 423 (1972).
(23) A. Kawaguchi, M. Ohara, and K. Kobayashi, *J. Macromol. Sci., -Phys., B*16, 193 (1979).
(24) M. Tasumi and S. Krimm, *J. Polymer Sci. Part A-2*, **6**, 995 (1968).
(25) R. E. Gilbert and K. Lonsdale, *Acta Cryst.*, **9**, 697 (1956).
(26) Y. Aoki, A. Chiba, and M. Kaneko, *J. Phys. Soc. Japan*, **27**, 1579 (1969).
(27) W. Schmidt and W. Vogel, *Colloid and Polymer Sci.*, **253**, 898 (1975).